

# Generalized Exponential Matrix Technique Application for the Evaluation of the Dispersion Characteristics of a Chiro-Ferrite Shielded Multilayered Microstrip Line

Samiha Daoudi<sup>1</sup>, Fatiha Benabdelaziz<sup>1</sup>, Chemseddine Zebiri<sup>2, \*</sup>, and Djamel Sayad<sup>3</sup>

**Abstract**—In this work, a new analytical matrix formulation approach for the characterization of a microwave planar structure printed on a complex medium is detailed. The approach is based on the Generalized Exponential Matrix Technique (GEMT) combined with the Method of Moments (MoM) and Galerkin's procedure. The mathematical calculation development is a robust approach that exclusively uses matrix formulations starting from Maxwell's equations until the derivation of a compact form of the Green's tensor of the studied structure. Reduced complexity and calculation simplicity foundation of the applied approach have actually incited the authors to consider the case study of a complex bianisotropic lossy chiral substrate medium. The complexity of the medium is expressed by full tensors form of all four constitutive parameters: permittivity, permeability and magnetoelectric parameters, each is represented by a nine-element tensor. To investigate the electromagnetic behavior of complex media, results of particular bianisotropy cases are presented and discussed. Original results of the biaxial chiral anisotropy case are carried out, discussed and compared with data available in literature.

## 1. INTRODUCTION

Since the first carried out research works on planar transmission lines in 1952, the microstrip line coplanar line and slot line have become the most known and commonly used planar transmission lines in microwave technology and microwave integrated circuits (MIC) devices [1]. Nowadays, transmission line-based microwave devices are largely used in telecommunication systems to constantly improve the overall performances by reducing the size, weight, and cost [2].

Microstrip lines are used at frequencies from a few megahertz to tens of gigahertz. Their fabrication technology offers at the same time simplicity and facility of realization and integration in microwave devices. Covered microstrips with air gap between the dielectric substrate and the ground plane present less losses than the conventional microstrip lines [3].

The Generalized Exponential Matrix Technique (GEMT) in the spectral domain is a rigorous method used to characterize the interaction of electromagnetic waves with bianisotropic multilayer structures. This technique, proposed by Tsalamengas [4], is used to study source radiations and wave propagation problems in multilayer structures with bianisotropic media [5]. This technique exhibits an elegant and systematic formulation. It has been developed by combining the Fourier transform with the matrix analysis method [6, 7].

In the last few years, the linear complex materials have gained much attention in electromagnetic applications. Among these materials the bianisotropic media, characterized by four independent constitutive tensors, are well mentioned. Theoretical research works have known an important progress

---

*Received 21 August 2017, Accepted 25 September 2017, Scheduled 9 October 2017*

\* Corresponding author: Chemseddine Zebiri (czebiri@univ-setif.dz).

<sup>1</sup> Department of Electronics, University Mentouri of Constantine-1, Constantine 25000, Algeria. <sup>2</sup> Department of Electronics, University Ferhat Abbas, Sétif-1-, 19000, Algeria. <sup>3</sup> Department of Electrical Engineering, 20 Aout 1955 University, Skikda 21000, Algeria.

dealing with their electromagnetic characterization and possibilities of potential applications of complex bianisotropic materials have greatly increased [6–8]. Complex media, such as magnetoelectric (ME) materials [9], have recently attracted much researcher attention. The ME effect [10] in complex materials is known as a product tensor property, which results from the cross interaction between different orderings of the two phases in the composite [10]. The chiral is considered as a complex medium. It is used as substrates and superstrates in the design of printed antennas [11]. The resolution of Maxwell's equations, in such structures, was not completely finished before 2001 [12]. Since then, the interaction of electromagnetic fields with chiral materials has been studied, in which the chiral medium is used in many applications, microstrip substrates and superstrates [13,14], and waveguides [15]. The propagation characterization in bianisotropic medium transmission lines have also prompted some interesting works [6,16].

In this study, we develop a GEMT-based mathematical formulation for a covered suspended bianisotropic substrate microstrip line using the MoM and the Galerkin's procedure in the spectral domain. The effect of the medium bianisotropy on the dispersion characteristics is presented and analyzed. Results are compared with the isotropic case reported in literature showing good agreements [16,17].

The novelty of this work lies in a complete matrix formulation of calculation development starting from Maxwell's equations until the derivation of the Green tensor avoiding any intermediate unnecessary calculations. In addition to the consideration of the losses in the dielectric substrate which have never been considered in previous works, this matrix formulation approach allows us to overcome excessive intermediate heavy calculations that are unnecessary in this approach which may lead to eventual mistakes.

## 2. THEORY

### 2.1. Constitutive Parameters of Chiro-Ferrite Media

The studied bianisotropic substrate microstrip line structure is presented in Fig. 1. The upper and lower layers (region 1 and 3) are isotropic dielectrics.

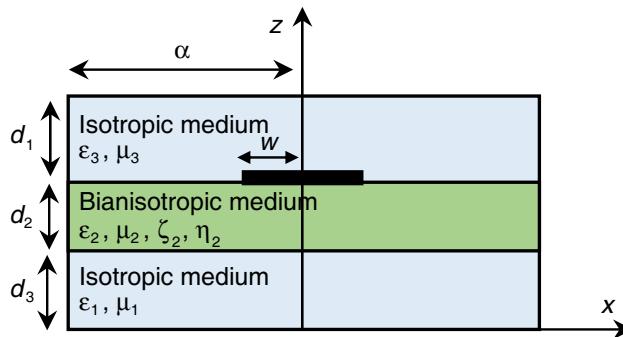


**Figure 1.** Geometry of the studied suspended microstrip line structure.

In general, bianisotropic media are characterized by the following constitutive relations [18].

$$\begin{aligned}\vec{B} &= [\mu]\vec{H} + ([\chi] + j[\xi])\sqrt{\mu_0\varepsilon_0}\vec{E} \\ \vec{D} &= [\varepsilon]\vec{E} + ([\chi] - j[\xi])\sqrt{\mu_0\varepsilon_0}\vec{H}\end{aligned}\quad (1a)$$

where  $\vec{E}$ ,  $\vec{H}$ ,  $\vec{D}$  and  $\vec{B}$  are the electric field, magnetic field, electric flux density and magnetic flux density, respectively.  $[\varepsilon]$  and  $[\mu]$  are the electric permittivity and magnetic permeability tensors, respectively.  $\varepsilon_0$  and  $\mu_0$  are the free space permittivity and permeability, respectively.  $[\chi]$  is the non-reciprocity (Tellegen), tensor and  $[\xi]$  is the chirality (Pasteur) tensor.

In fact, this study is based on a Pasteur and Tellegen medium, which is a general anisotropic chiral, (i.e.,  $[\chi] = 0$  and  $[\xi] \neq 0$  [18] or  $[\chi] \neq 0$  and  $[\xi] = 0$ ).

The linear stationary dispersive bianisotropic materials can be described by the following constitutive relations in the frequency domain

$$\begin{aligned}\vec{D} &= \varepsilon_0 [\varepsilon(\omega)] \vec{E} + \sqrt{\varepsilon_0 \mu_0} [\xi(\omega)] \vec{H} \\ \vec{B} &= \mu_0 [\mu(\omega)] \vec{H} + \sqrt{\varepsilon_0 \mu_0} [\eta(\omega)] \vec{E}\end{aligned}\tag{1b}$$

where the time dependence ( $e^{j\omega t}$ ) is assumed. In the Cartesian coordinate system, the tensors of the relative permittivity  $[\varepsilon(\omega)]$  and relative permeability  $[\mu(\omega)]$  are given by:

$$[\varepsilon(\omega)] = \begin{bmatrix} \varepsilon_{xx} & \varepsilon_{xy} & \varepsilon_{xz} \\ \varepsilon_{yx} & \varepsilon_{yy} & \varepsilon_{yz} \\ \varepsilon_{zx} & \varepsilon_{zy} & \varepsilon_{zz} \end{bmatrix}, \quad [\mu(\omega)] = \begin{bmatrix} \mu_{xx} & \mu_{xy} & \mu_{xz} \\ \mu_{yx} & \mu_{yy} & \mu_{yz} \\ \mu_{zx} & \mu_{zy} & \mu_{zz} \end{bmatrix}\tag{2a}$$

and the magnetoelectric tensors  $[\xi(\omega)]$  and  $[\eta(\omega)]$  are given by:

$$[\xi(\omega)] = \begin{bmatrix} \xi_{xx} & \xi_{xy} & \xi_{xz} \\ \xi_{yx} & \xi_{yy} & \xi_{yz} \\ \xi_{zx} & \xi_{zy} & \xi_{zz} \end{bmatrix}, \quad [\eta(\omega)] = \begin{bmatrix} \eta_{xx} & \eta_{xy} & \eta_{xz} \\ \eta_{yx} & \eta_{yy} & \eta_{yz} \\ \eta_{zx} & \eta_{zy} & \eta_{zz} \end{bmatrix}\tag{2b}$$

The bianisotropic medium is a generalization of the anisotropic and chiral media [19]. Different types of anisotropic media are possible: uniaxial, biaxial, gyrotropic, . . . , as it is possible to have only one nonzero element of the nine-element matrix [20]. In [14] and [21], a special case of the above magnetoelectric elements was treated. An important step in the distinction between anisotropic media comes through splitting the constitutive parameter dyadic matrix  $x$  ( $x = \varepsilon, \mu, \xi$  and  $\eta$ ) into two parts, symmetric and antisymmetric [22].

$$x = \begin{bmatrix} x_x & x_{xy} & x_{xz} \\ x_{yx} & x_y & x_{yz} \\ x_{zx} & x_{zy} & x_z \end{bmatrix} = \underbrace{\begin{bmatrix} x_x & 0 & 0 \\ 0 & x_y & 0 \\ 0 & 0 & x_z \end{bmatrix}}_{\text{symmetric} \rightarrow \text{uniaxial, biaxial anisotropy}} + \underbrace{\begin{bmatrix} 0 & x_{xy} & x_{xz} \\ x_{yx} & 0 & x_{yz} \\ x_{zx} & x_{zy} & 0 \end{bmatrix}}_{\text{antisymmetric} \rightarrow \text{gyrotropic anisotropy}}\tag{3a}$$

This can be simplified into:

$$x = \underbrace{x_x \bar{u}_x \bar{u}_x + x_y \bar{u}_y \bar{u}_y + x_z \bar{u}_z \bar{u}_z}_{\text{symmetric}} + \underbrace{x_g \bar{u}_z \times I}_{\text{antisymmetric}}\tag{3b}$$

where:

$$x_g = \begin{bmatrix} 0 & x_{xy} & x_{xz} \\ x_{yx} & 0 & x_{yz} \\ x_{zx} & x_{zy} & 0 \end{bmatrix}\tag{3c}$$

and  $I$  is the unit dyadic matrix.

The symmetric part of the dyad “ $x$ ” has a principal axis along  $x, y$  or  $z$  direction, and these elements determine the uniaxial and biaxial anisotropy. The other elements  $x_g$  (antisymmetric) define the gyrotropic anisotropy of the medium. When all the constitutive parameters are scalar, the medium is said to be biisotropic.

According to the gyrotropic bianisotropy of constitutive parameters  $\xi$  and  $\eta$ , it is possible to define several medium types, depending on the form of the constitutive tensors in Equation (2). Some cases of linear complex media are considered in [23–28]; in [24, 25], two cases:  $\xi = \eta = 0$  and  $\xi = -\eta$ , in [23–27], the case:  $\xi = \eta \neq 0$ , and in [24, 28] the case:  $\xi \neq \eta$ .

## 2.2. Matrix Formulation

Calculation developments, starting from Maxwell’s equations and using the spectral domain GEMT, lead to a 1st order differential equation for the transverse electromagnetic field components as functions of their derivatives in the  $i$ th region [6]:

$$\frac{\partial [\tilde{f}^{(i)}(\alpha, \beta, z)]}{\partial z} = [\mathbf{P}^{(i)}]_{4 \times 4} [\tilde{f}^{(i)}(\alpha, \beta, z)]\tag{4a}$$

and:

$$\left[ \tilde{f}^{(i)}(\alpha, \beta, z) \right] = \begin{bmatrix} \tilde{E}_x^{(i)}(\alpha, \beta, z) \\ \tilde{E}_y^{(i)}(\alpha, \beta, z) \\ \tilde{H}_x^{(i)}(\alpha, \beta, z) \\ \tilde{H}_y^{(i)}(\alpha, \beta, z) \end{bmatrix} \quad (4b)$$

$$[\mathbf{P}] = j\kappa_0 \{ [\mathbf{A}] + [\mathbf{B}][\mathbf{C}][\mathbf{D}] \} \quad (4c)$$

where

$$[\mathbf{A}] = \begin{bmatrix} -\eta_{yx} & -\eta_{yy} & -Z_0\mu_{yx} & -Z_0\mu_{yy} \\ \eta_{xx} & \eta_{xy} & Z_0\mu_{xx} & Z_0\mu_{xy} \\ \Upsilon_0\varepsilon_{yx} & \Upsilon_0\varepsilon_{yy} & \xi_{yx} & \xi_{yy} \\ -\Upsilon_0\varepsilon_{xx} & -\Upsilon_0\varepsilon_{xy} & -\xi_{xx} & -\xi_{xy} \end{bmatrix} = \begin{bmatrix} [\eta_T] & Z_0[\mu_T] \\ -\Upsilon_0[\varepsilon_T] & -[\xi_T] \end{bmatrix} \quad (4d)$$

$$[\mathbf{B}] = \begin{bmatrix} -j(\kappa_0\eta_{yz} + \kappa_x) & -j\omega\mu_0\mu_{yz} \\ j(\kappa_0\eta_{xz} - \kappa_y) & j\omega\mu_0\mu_{xz} \\ j\omega\varepsilon_0\varepsilon_{yz} & j(\kappa_0\xi_{yz} - \kappa_x) \\ -j\omega\varepsilon_0\varepsilon_{xz} & -j(\kappa_0\xi_{xz} + \kappa_y) \end{bmatrix} = \begin{bmatrix} -(\eta_{yz} + \kappa_x^n) & -Z_0\mu_{yz} \\ (\eta_{xz} - \kappa_y^n) & Z_0\mu_{xz} \\ \Upsilon_0\varepsilon_{yz} & (\xi_{yz} - \kappa_x^n) \\ -\Upsilon_0\varepsilon_{xz} & -(\xi_{xz} + \kappa_y^n) \end{bmatrix} \quad (4e)$$

$$[\mathbf{C}] = \frac{-1}{(\varepsilon_{zz}\mu_{zz} - \xi_{zz}\eta_{zz})} \begin{bmatrix} Z_0\mu_{zz} & \xi_{zz} \\ -\eta_{zz} & -\Upsilon_0\varepsilon_{zz} \end{bmatrix} \quad (4f)$$

$$[\mathbf{D}] = \begin{bmatrix} \Upsilon_0\varepsilon_{xz} & \Upsilon_0\varepsilon_{yz} & (\xi_{xz} - \kappa_y^n) & (\xi_{yz} + \kappa_x^n) \\ -(\eta_{xz} + \kappa_y^n) & -(\eta_{yz} - \kappa_x^n) & -Z_0\mu_{xz} & -Z_0\mu_{yz} \end{bmatrix} \quad (4g)$$

where  $\kappa_x^n = \frac{\kappa_x}{\kappa_0}$  and  $\kappa_y^n = \frac{\kappa_y}{\kappa_0}$  are the normalized  $x$  and  $y$  wavenumber components, and  $Z_0 = \frac{1}{\Upsilon_0} = \sqrt{\frac{\mu_0}{\varepsilon_0}}$  is the free space characteristic impedance.

$[\mathbf{P}]$  denotes a  $z$ -independent matrix. In all previous works [6, 7], matrix  $\mathbf{P}$  is calculated explicitly, while in this study it is kept in its matrix form, where the elements are derived from the constitutive relations. This matrix is the first form which characterizes the medium in our matrix formulation study. The elements of such a matrix are not necessarily developed; the matrix is inserted in its raw form. The general solution of Equation (4a) is given by:

$$\begin{bmatrix} E_x(z) \\ E_y(z) \\ H_x(z) \\ H_y(z) \end{bmatrix} = \exp([\mathbf{P}] \cdot z) \begin{bmatrix} E_x(0) \\ E_y(0) \\ H_x(0) \\ H_y(0) \end{bmatrix} \quad (5)$$

which has a general solution of the form:

$$\begin{bmatrix} E_x(z) \\ E_y(z) \\ H_x(z) \\ H_y(z) \end{bmatrix} = \mathbf{T}(\kappa_x, \kappa_y, z) \begin{bmatrix} E_x(0) \\ E_y(0) \\ H_x(0) \\ H_y(0) \end{bmatrix} \quad (6a)$$

and

$$\tilde{f}^{(i)}(\alpha, \beta, z(i)) = \mathbf{T}(\kappa_x, \kappa_y, z) \tilde{f}^{(i)}(\alpha, \beta, z(i-1)) \quad (6b)$$

According to Cayley-Hamilton theorem, the transition matrix is expressed under the following form

$$\mathbf{T}(z) = c_0\mathbf{I} + c_1\mathbf{P} + c_2\mathbf{P}^2 + c_3\mathbf{P}^3. \quad (7)$$

where  $c_j$  ( $j = 0, 1, 2, 3$ ) are scalar expansion coefficients that can be given by solving the Vandermode linear algebraic system. According to Equation (6a), we realize the advantage of using this technique. We notice that it is sufficient to know the transition matrices  $\mathbf{T}(\kappa_x, \kappa_y, z)$  of the structure limit (upper and lower) layers. Multiplying the layers transition matrices and applying the boundary conditions between the dielectric layers containing the conductors give the Green's tensor which models the structure.

$\mathbf{T}(\kappa_x, \kappa_y, z)$  is calculated in the formulation of the GEMT by means of the Cayley Hamilton theorem in conjunction with Muller's method to determine the complex function roots.

Muller's method is a generalization of the secant method used to find real or complex zeros of a function and is an iterative method which requires three starting points  $(p, f(p))$ ,  $(p_1, f(p_1))$ , and  $(p_2, f(p_2))$ . A parabola is made to fit the three points, then a quadratic formula is used to find a root of the quadratic approximation for the next root. It is shown that close to a root Muller's method converges more quickly than the secant method and almost as quickly as the Newton method.

### 2.3. Boundary Conditions and Green's Matrix Tensor Evaluation

According to the conditions in the vicinity of a perfect conductor, the electric and magnetic field components for regions  $z \subseteq [0, d_1]$  and  $z \subseteq [d_2, d_3]$  are:

$$\begin{bmatrix} E_x(z) \\ E_y(z) \\ H_x(z) \\ H_y(z) \end{bmatrix} = f^{(1)}(\alpha, \beta, z) = [\mathbf{L}_1] \begin{bmatrix} \tilde{C}_1 \\ \tilde{C}_4 \end{bmatrix} \quad (8a)$$

$$\begin{bmatrix} E_x(z) \\ E_y(z) \\ H_x(z) \\ H_y(z) \end{bmatrix} = f^{(3)}(\alpha, \beta, z) = [\mathbf{L}_3] \begin{bmatrix} \tilde{C}_2 \\ \tilde{C}_3 \end{bmatrix} \quad (8b)$$

with

$$[\mathbf{L}_1] = \begin{bmatrix} -\frac{\alpha_n \gamma_0}{\omega \varepsilon_0} & j\beta \\ -\frac{\beta \gamma_0}{\omega \varepsilon_0} & -j\alpha_n \\ -j\beta \coth(\gamma_0 d_1) & -\frac{\alpha_n \gamma_0}{\omega \mu_0} \coth(\gamma_0 d_1) \\ j\alpha_n \coth(\gamma_0 d_1) & -\frac{\beta}{\omega \mu_0} \coth(\gamma_0 d_1) \end{bmatrix} \quad (8c)$$

$$[\mathbf{L}_3] = \begin{bmatrix} \frac{\alpha_n \gamma_0}{\omega \varepsilon_0} & j\beta \\ \frac{\beta \gamma_0}{\omega \varepsilon_0} & -j\alpha_n \\ -j\beta \coth(\gamma_0 d_3) & \frac{\alpha_n \gamma_0}{\omega \mu_0} \coth(\gamma_0 d_3) \\ j\alpha_n \coth(\gamma_0 d_3) & \frac{\beta}{\omega \mu_0} \coth(\gamma_0 d_3) \end{bmatrix} \quad (8d)$$

and

$$\tilde{C}_1 = C_1 \sinh(\gamma_0 d_1) \quad (8e)$$

$$\tilde{C}_2 = C_2 \sinh(\gamma_0 d_3) \quad (8f)$$

$$\tilde{C}_3 = C_3 \sinh(\gamma_0 d_3) \quad (8g)$$

$$\tilde{C}_4 = C_4 \sinh(\gamma_0 d_1) \quad (8h)$$

Applying the general solution of the GEMT and enforcing the boundary conditions imposed by the conducting strips, we get:

$$\begin{bmatrix} \tilde{E}_x^{(3)} \\ \tilde{E}_y^{(3)} \\ \tilde{H}_x^{(3)} \\ \tilde{H}_y^{(3)} \end{bmatrix} - \begin{bmatrix} \tilde{E}_x^{(2)} \\ \tilde{E}_y^{(2)} \\ \tilde{H}_x^{(2)} \\ \tilde{H}_y^{(2)} \end{bmatrix} = \begin{bmatrix} 0 \\ 0 \\ -\tilde{J}_y^{(2)} \\ \tilde{J}_x^{(2)} \end{bmatrix} \quad (9)$$

According to Equation (9), we obtain the matrix equation which relates the transverse components of the electric and magnetic fields to the transverse current densities [6].

$$[\mathbf{T}] [\mathbf{L}_1] \begin{bmatrix} \tilde{C}_1 \\ \tilde{C}_4 \end{bmatrix} = [\mathbf{L}_3] \begin{bmatrix} \tilde{C}_2 \\ \tilde{C}_3 \end{bmatrix} + \begin{bmatrix} 0 \\ 0 \\ \tilde{J}_y \\ -\tilde{J}_x \end{bmatrix} \quad (10a)$$

$$[\mathbf{L}]_{(4,2)} = [\mathbf{T}] \cdot [\mathbf{L}_1]_{(4,2)} \quad (10b)$$

$$[\mathbf{L}]_{(4,2)} \cdot \begin{bmatrix} \tilde{C}_1 \\ \tilde{C}_4 \end{bmatrix} = [\mathbf{L}_3]_{(4,2)} \cdot \begin{bmatrix} \tilde{C}_2 \\ \tilde{C}_3 \end{bmatrix} + \begin{bmatrix} 0 \\ 0 \\ \tilde{J}_y \\ -\tilde{J}_x \end{bmatrix}. \quad (10c)$$

We denote by  $[\mathbf{L}]$  and  $[\mathbf{L}_3]$  the transfer matrices for the structures which contain the layers with  $(0 \leq z \leq d_1)$  and  $(d_2 \leq z \leq d_3)$ .

$$[\mathbf{FM}] \begin{bmatrix} \tilde{C}_1 \\ \tilde{C}_4 \\ \tilde{C}_2 \\ \tilde{C}_3 \end{bmatrix} = \begin{bmatrix} 0 \\ 0 \\ \tilde{J}_y \\ -\tilde{J}_x \end{bmatrix} \quad (11a)$$

$$[\mathbf{FM}]_{(4,4)} = [\mathbf{L}_{(4,2)} \mathbf{L}_{3(4,2)}] \quad (11b)$$

Using Cramer's rule for the determination of the constants obtained by enforcing the boundary conditions in the air-dielectric interface, we get the following matrix form for these constants:

$$[\mathbf{C}_1] = \begin{bmatrix} FM(1,1) & FM(1,2) & FM(1,4) \\ FM(2,1) & FM(2,2) & FM(2,4) \\ FM(4,1) & FM(4,2) & FM(4,4) \end{bmatrix} \quad (12a)$$

$$[\mathbf{C}_2] = \begin{bmatrix} FM(1,1) & FM(1,2) & FM(1,4) \\ FM(2,1) & FM(2,2) & FM(2,4) \\ FM(3,1) & FM(3,2) & FM(3,4) \end{bmatrix} \quad (12b)$$

$$[\mathbf{C}_3] = \begin{bmatrix} FM(1,1) & FM(1,2) & FM(1,3) \\ FM(2,1) & FM(2,2) & FM(2,3) \\ FM(4,1) & FM(4,2) & FM(4,3) \end{bmatrix} \quad (12c)$$

$$[\mathbf{C}_4] = \begin{bmatrix} FM(1,1) & FM(1,2) & FM(1,3) \\ FM(2,1) & FM(2,2) & FM(2,3) \\ FM(3,1) & FM(3,2) & FM(4,3) \end{bmatrix} \quad (12d)$$

where  $[\mathbf{C}_1]$  is obtained by deleting the 3<sup>rd</sup> row and 3<sup>rd</sup> column of  $[\mathbf{FM}]_{(4,4)}$ ,  $[\mathbf{C}_2]$  obtained by deleting the 4<sup>th</sup> row and 3<sup>rd</sup> column of  $[\mathbf{FM}]_{(4,4)}$ ,  $[\mathbf{C}_3]$  obtained by deleting the 3<sup>rd</sup> row and 4<sup>th</sup> column of  $[\mathbf{FM}]_{(4,4)}$ ,  $[\mathbf{C}_4]$  obtained by deleting the 4<sup>th</sup> row and 4<sup>th</sup> column of  $[\mathbf{FM}]_{(4,4)}$ , and  $[\mathbf{C}_1]$  obtained by deleting the 3<sup>rd</sup> row and 3<sup>rd</sup> column of  $[\mathbf{FM}]_{(4,4)}$ .

This matrix formulation exhibits a compact form with the advantage of being easily integrated in the calculation code.

At the air-dielectric interface  $z = d_2$ , the continuity of the field tangential components has to be satisfied. By determining the expressions of the constants  $[\mathbf{C}_1]$ ,  $[\mathbf{C}_2]$ ,  $[\mathbf{C}_3]$  and  $[\mathbf{C}_4]$ , the expressions of the electric and magnetic fields are evaluated at the interface air-dielectric. Hence, the novel matrix form of the elements of the Green tensor  $G_{ij}(\alpha_n, \gamma)$  is obtained according to the following system of equations.

$$\tilde{E}_x = G_{11}(\alpha_n, \gamma) \tilde{j}_x + G_{12}(\alpha_n, \gamma) \tilde{j}_y \quad (13a)$$

$$\tilde{E}_y = G_{21}(\alpha_n, \gamma) \tilde{j}_x + G_{22}(\alpha_n, \gamma) \tilde{j}_y \quad (13b)$$

where

$$G_{11}(\alpha_n, \gamma) = \left( \frac{L(1,1) \cdot \Delta[\mathbf{C}_2] - L(1,2) \cdot \Delta[\mathbf{C}_4]}{\Delta} \right) \quad (13c)$$

$$G_{12}(\alpha_n, \gamma) = \left( \frac{L(1,1) \cdot \Delta[\mathbf{C}_1] - L(1,2) \cdot \Delta[\mathbf{C}_3]}{\Delta} \right) \quad (13d)$$

$$G_{21}(\alpha_n, \gamma) = \left( \frac{L(2,1) \cdot \Delta[\mathbf{C}_2] - L(2,2) \cdot \Delta[\mathbf{C}_4]}{\Delta} \right) \quad (13e)$$

$$G_{22}(\alpha_n, \gamma) = \left( \frac{L(2,1) \cdot \Delta[\mathbf{C}_1] - L(2,2) \cdot \Delta[\mathbf{C}_3]}{\Delta} \right) \quad (13f)$$

where  $\Delta$  is the determinant of  $[\mathbf{FM}]_{(4,4)}$ .

#### 2.4. Resolution of the System

By enforcing the boundary conditions imposed on the field components and the current distributions at the air-dielectric interface, the integral equations are converted into a homogeneous system of linear equations. The resolution of the equation  $\det(\gamma) = 0$  is carried out using the spectral domain MoM and Galerkin's procedure [6, 8, 17]. For lossy media, a complex propagation constant  $\gamma = \alpha + j\beta$  is expected.

### 3. RESULTS AND DISCUSSION

#### 3.1. Validation of Results

Figures 2 and 3 show the case study of 2 and 3-layer structures (Fig. 1) compared with results reported in literature [16, 29]. Our obtained results are in good agreement with the studied cases. A slight shift that does not exceed 8% is observed which is mainly due to the consideration of the dielectric losses.

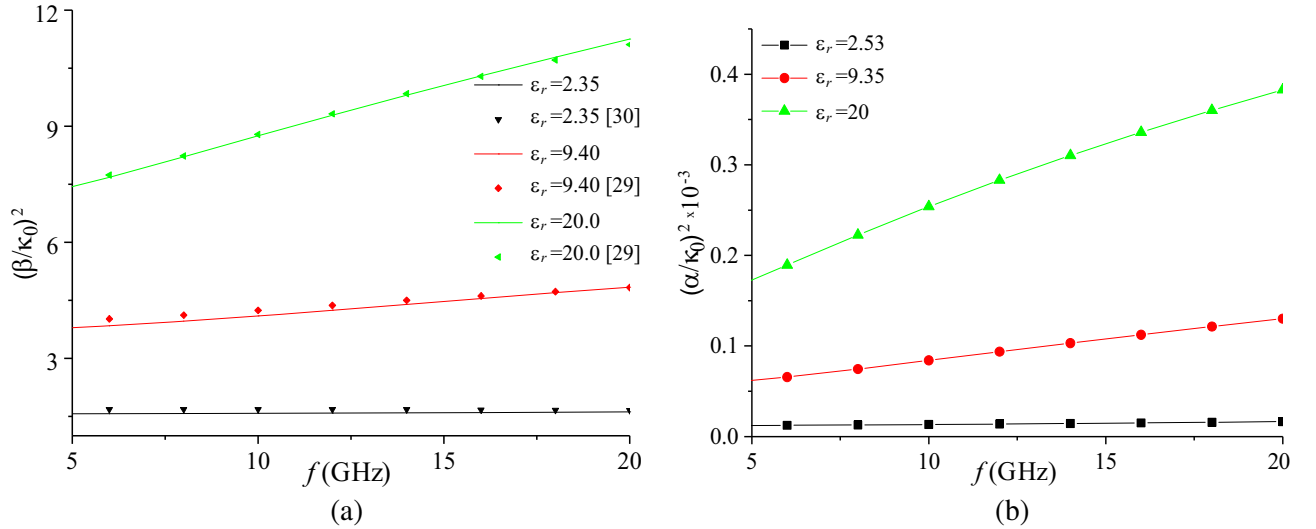


**Figure 2.** (a)  $(\frac{\beta}{\kappa_0})^2$  ratio, and (b)  $(\frac{\alpha}{\kappa_0})^2$  ratio of the suspended microstrip line structure for different values of  $\epsilon_r$ . ( $a = 10$  mm,  $d_1 = 4.5$  mm,  $d_2 = 1$  mm,  $d_3 = 4.5$  mm,  $w = 1$  mm).

In this study, we take into account the losses combined with the chiral medium with a biaxial anisotropy, a case that has never been treated in literature. Original results are obtained and discussed for the case of a monolayer structure.

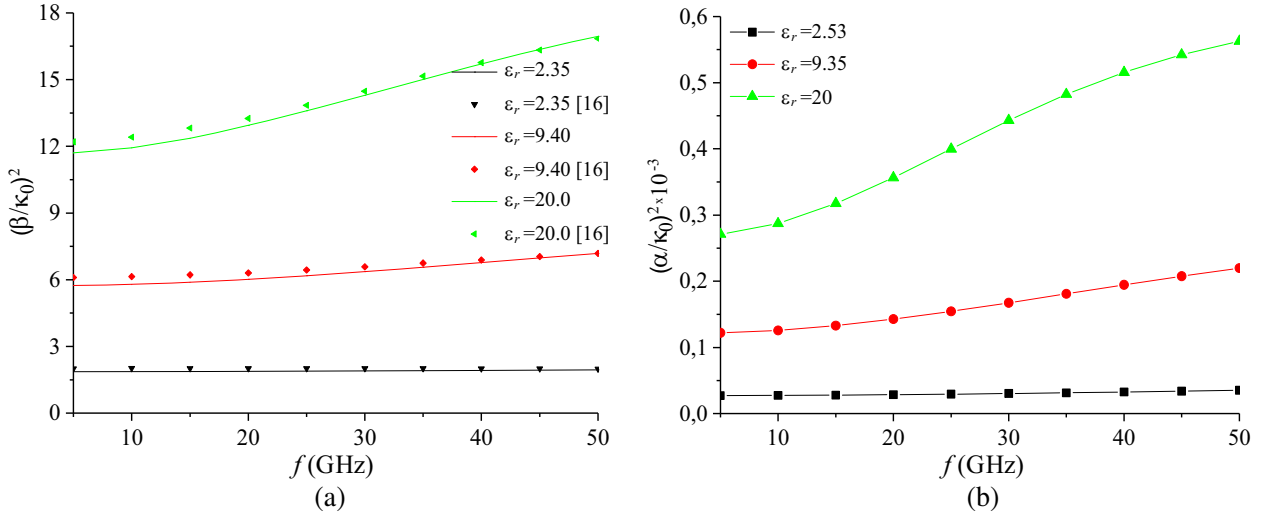


**Figure 3.** (a)  $(\frac{\beta}{\kappa_0})^2$  ratio, and (b)  $(\frac{\alpha}{\kappa_0})^2$  ratio of the microstrip for different values of  $\epsilon_r$ . ( $a = 12.7$  mm,  $d_1 = 11.43$  mm,  $d_2 = 0.5$  mm,  $d_3 = 0$  mm,  $w = 0.5$  mm).

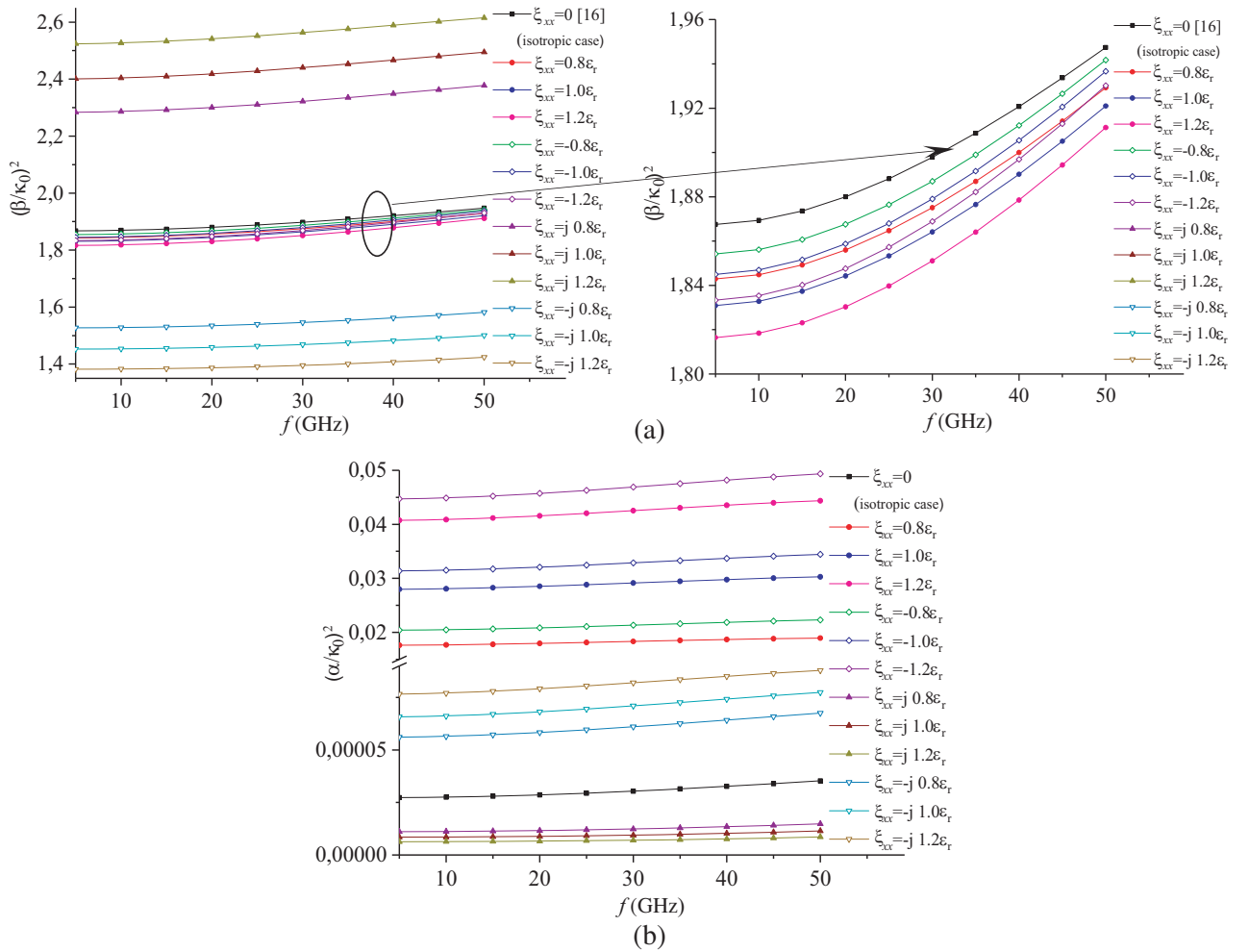


**Figure 4.** Effect of the chirality  $\xi_{xx}$  on the (a)  $(\frac{\beta}{\kappa_0})^2$  ratio and (b)  $(\frac{\alpha}{\kappa_0})^2$  ratio of the microstrip. ( $a = 12.7$  mm,  $d_1 = 11.43$  mm,  $d_2 = 0.5$  mm,  $d_3 = 0$  mm,  $w = 0.5$  mm,  $\epsilon_r = 2.53$ ).



### 3.2. Effect of the Chirality on the Complex Propagation Constant

The following figures present the effect of the chirality parameter  $\xi$  and  $\eta$  of a monolayer microstrip line structure ( $d_3 = 0$  mm in Fig. 1). Initially we examine the effect of the axial chirality element by element.

The values of the magnetoelectric elements, whether they are real or imaginary, positive or negative, directly affect the effective constant as well as the losses.

According to Fig. 4(a), the notion of non-reciprocity is remarkable when changing the sign of the purely imaginary magnetoelectric element  $\xi_{xx}$ , with an increase in  $(\beta/\kappa_0)^2$  when imaginary positive-valued  $\xi_{xx}$  increases and a decrease when imaginary negative-valued  $\xi_{xx}$  decreases. This effect reversed with respect to  $(\alpha/\kappa_0)^2$  parameter, which is clearly illustrated by Fig. 4(c).

The increase in real values of  $\xi_{xx}$  leads to a slight decrease in  $(\beta/\kappa_0)^2$  and a significant increase in the ratio  $(\alpha/\kappa_0)^2$  (Figs. 4(a) and (b)). Real positive values of  $\xi_{xx}$  have more effect than negative ones;

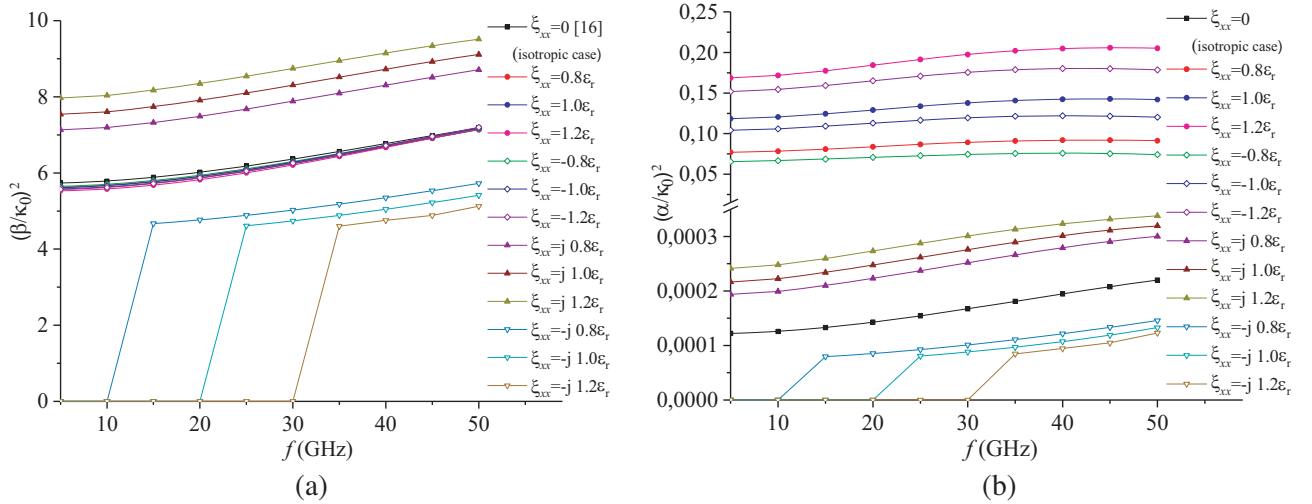


**Figure 5.** Effect of the chirality  $\xi_{xx}$  on (a) the  $(\frac{\beta}{\kappa_0})^2$  ratio and (b) the  $(\frac{\alpha}{\kappa_0})^2$  ratio of the microstrip. ( $a = 12.7$  mm,  $d_1 = 11.43$  mm,  $d_2 = 0.5$  mm,  $d_3 = 0$  mm,  $w = 0.5$  mm,  $\epsilon_r = 9.4$ ).

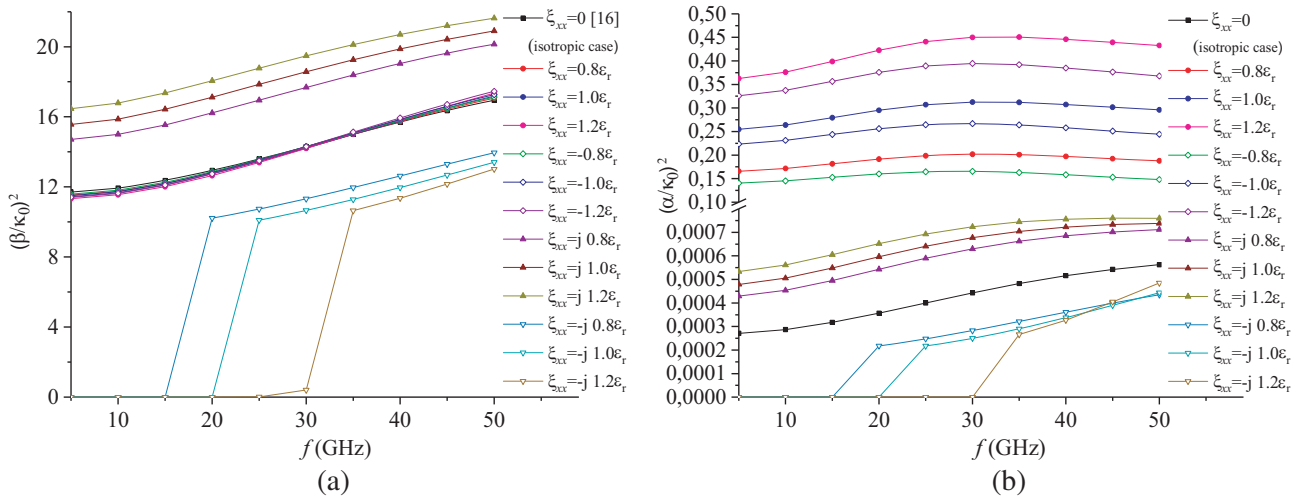


**Figure 6.** Effect of the chirality  $\xi_{xx}$  on (a) the  $(\frac{\beta}{\kappa_0})^2$  ratio and (b) the  $(\frac{\alpha}{\kappa_0})^2$  ratio of the microstrip. ( $a = 12.7$  mm,  $d_1 = 11.43$  mm,  $d_2 = 0.5$  mm,  $d_3 = 0$  mm,  $w = 0.5$  mm,  $\epsilon_r = 20$ ).

these effects on  $(\alpha/\kappa_0)^2$  and  $(\beta/\kappa_0)^2$  are reversed with respect to the sign of the parameter  $\xi_{xx}$ .

Figs. 4, 5 and 6 illustrate the effect of chirality for  $\varepsilon_r = 2.53$ , 9.4 and 20, respectively. We observe that the increase in  $\varepsilon_r$  induces an increase in the chirality effect ( $\xi_{xx}$  is kept constant) on both  $(\alpha/\kappa_0)^2$  and  $(\beta/\kappa_0)^2$  parameters. In particular, for a negative imaginary magnetoelectric element, we observe a delayed appearance of the fundamental mode increasingly with the increase  $\varepsilon_r$  (5 GHz for  $\varepsilon_r = 2.53$ , 15 GHz for  $\varepsilon_r = 9.4$  and 20 GHz for  $\varepsilon_r = 20$ ). The effective permittivity starts approximately from the reference (isotropic case  $+ \cong [0.5 * (\varepsilon_r + 1) + \Delta f(\varepsilon_r, \xi_{xx})]$ ) in all treated cases.

Regarding the magnetoelectric element  $\xi_{yy}$  (Fig. 7), its effect on the parameters  $(\alpha/\kappa_0)^2$  and  $(\beta/\kappa_0)^2$  is insignificant, due to the choice of the geometrical orientation of the treated structure (Fig. 1). Figs. 8 and 9 present the combined effect of  $\xi_{zz}$  with  $\varepsilon_r = 2.53$  and 9.4, respectively, which is marked by almost identical effects relative to  $\xi_{zz}$ . The magnetoelectric elements  $\eta_{zz}$  have the same effect as that of parameter  $(-\xi_{zz})$  as illustrated by Figs. 10, 11 and 12.

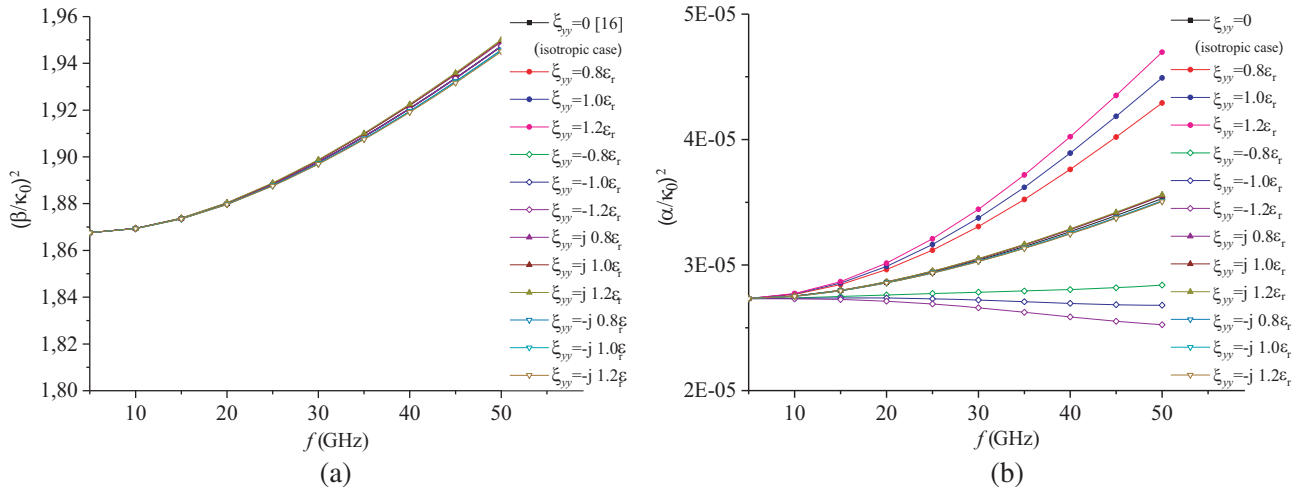


**Figure 7.** Effect of the chirality  $\xi_{yy}$  on (a) the  $(\frac{\beta}{\kappa_0})^2$  ratio and (b) the  $(\frac{\alpha}{\kappa_0})^2$  ratio of the microstrip. ( $a = 12.7$  mm,  $d_1 = 11.43$  mm,  $d_2 = 0.5$  mm,  $d_3 = 0$  mm,  $w = 0.5$  mm,  $\varepsilon_r = 2.53$ ).

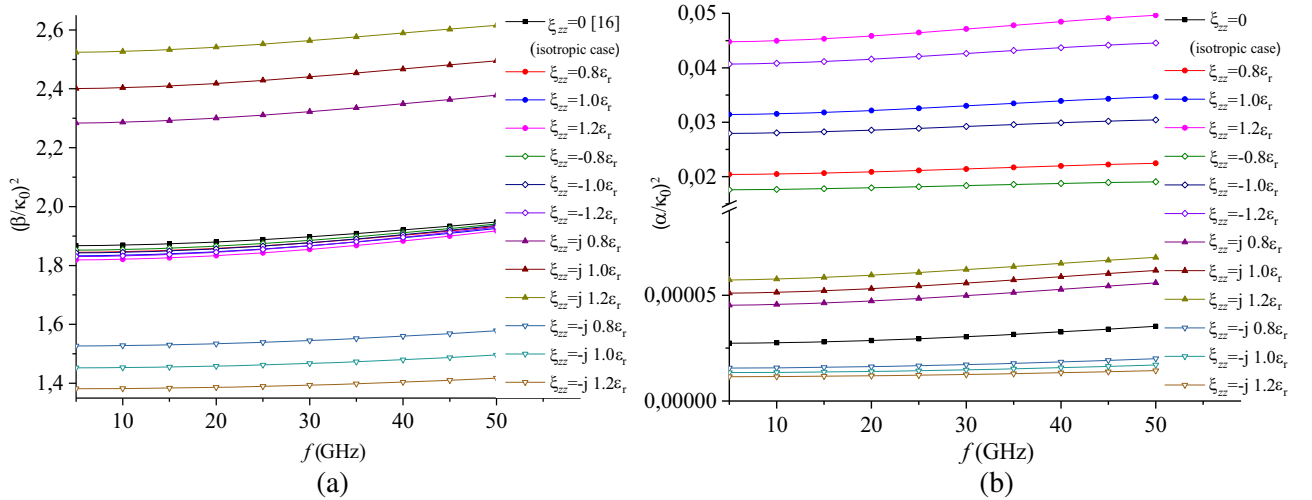


**Figure 8.** Effect of the chirality  $\xi_{zz}$  on (a) the  $(\frac{\beta}{\kappa_0})^2$  ratio and (b) the  $(\frac{\alpha}{\kappa_0})^2$  ratio of the microstrip. ( $a = 12.7$  mm,  $d_1 = 11.43$  mm,  $d_2 = 0.5$  mm,  $d_3 = 0$  mm,  $w = 0.5$  mm,  $\varepsilon_r = 2.53$ ).

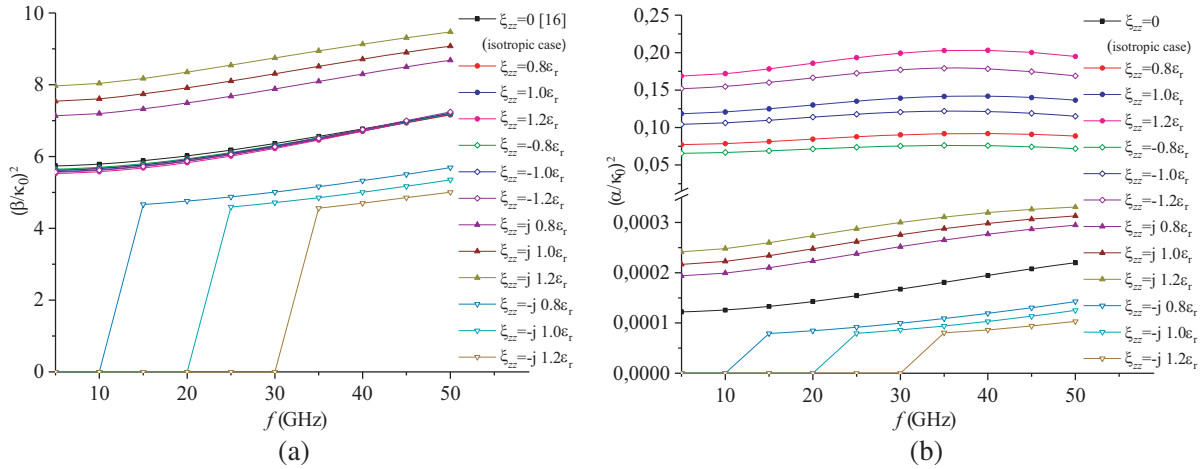


**Figure 9.** Effect of the chirality  $\xi_{zz}$  on (a) the  $(\frac{\beta}{\kappa_0})^2$  ratio and (b) the  $(\frac{\alpha}{\kappa_0})^2$  ratio of the microstrip. ( $a = 12.7$  mm,  $d_1 = 11.43$  mm,  $d_2 = 0.5$  mm,  $d_3 = 0$  mm,  $w = 0.5$  mm,  $\epsilon_r = 9.4$ ).

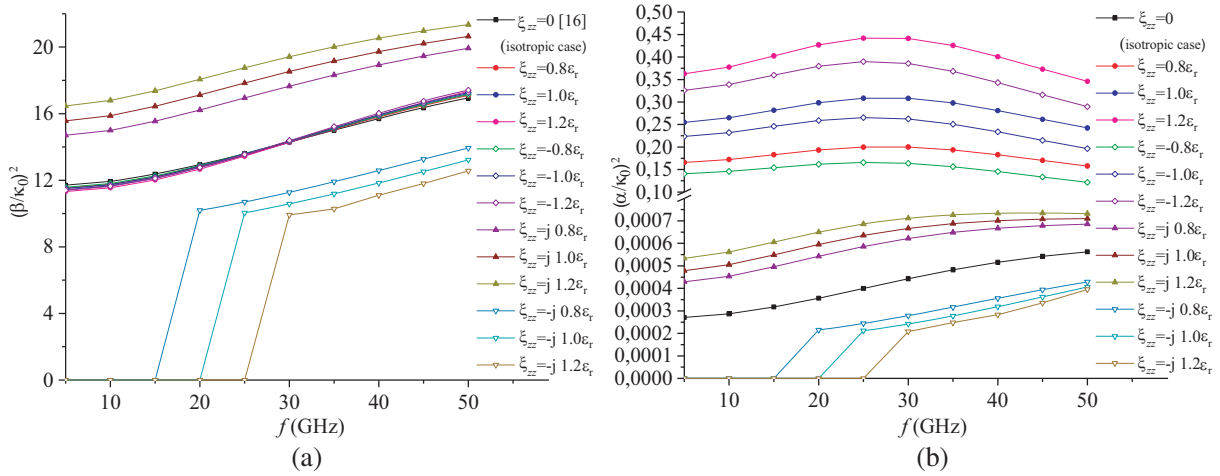


**Figure 10.** Effect of the chirality  $\xi_{zz}$  on (a) the  $(\frac{\beta}{\kappa_0})^2$  ratio and (b) the  $(\frac{\alpha}{\kappa_0})^2$  ratio of the microstrip. ( $a = 12.7$  mm,  $d_1 = 11.43$  mm,  $d_2 = 0.5$  mm,  $d_3 = 0$  mm,  $w = 0.5$  mm,  $\epsilon_r = 20$ ).

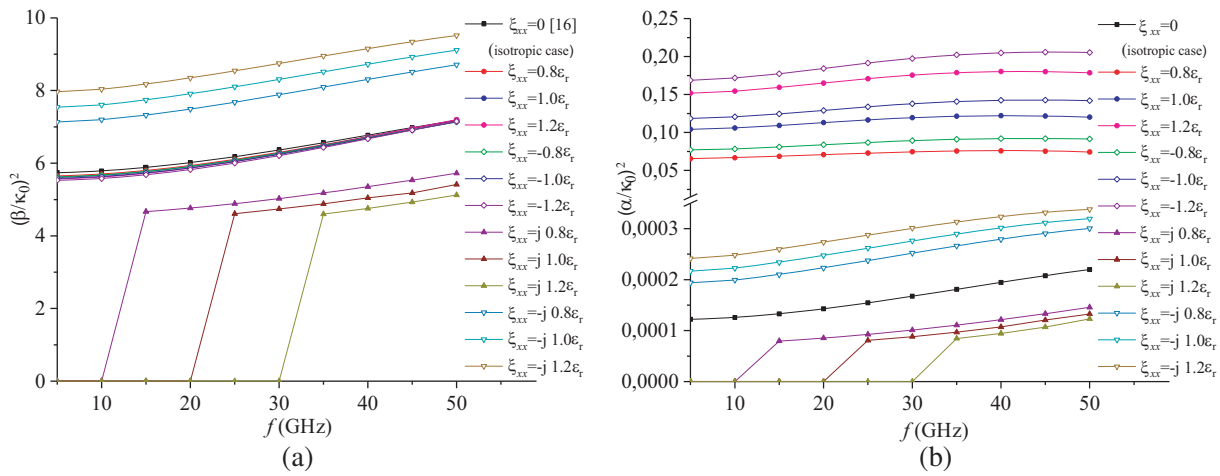


**Figure 11.** Effect of the chirality  $\eta_{xx}$  on (a) the  $(\frac{\beta}{\kappa_0})^2$  ratio and (b) the  $(\frac{\alpha}{\kappa_0})^2$  ratio of the microstrip. ( $a = 12.7$  mm,  $d_1 = 11.43$  mm,  $d_2 = 0.5$  mm,  $d_3 = 0$  mm,  $w = 0.5$  mm,  $\epsilon_r = 9.4$ ).

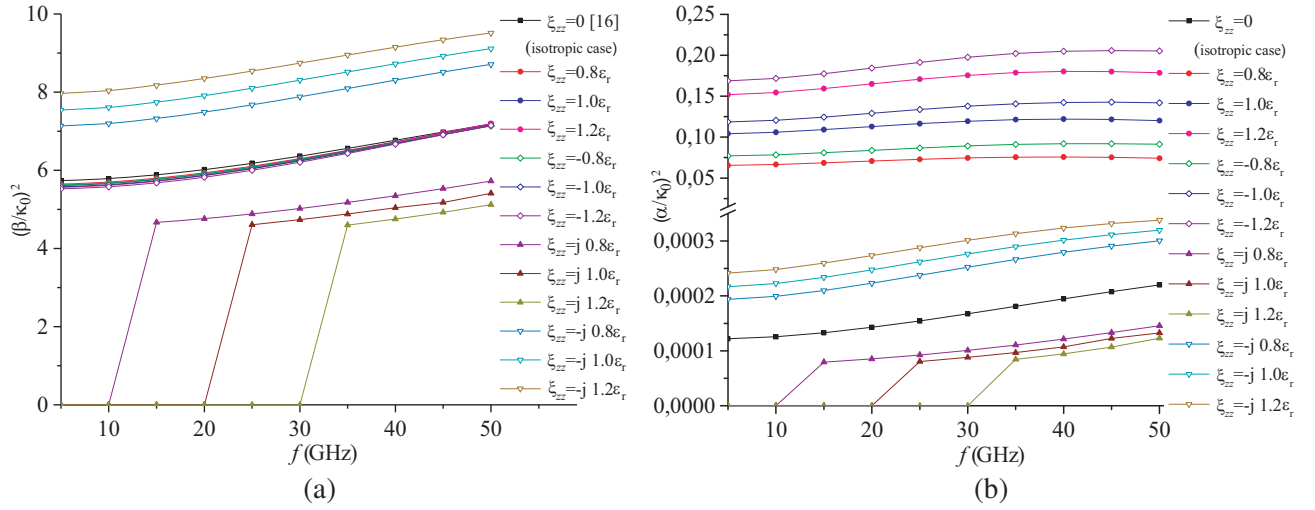


**Figure 12.** Effect of the chirality  $\eta_{zz}$  on (a) the  $(\frac{\beta}{\kappa_0})^2$  ratio and (b) the  $(\frac{\alpha}{\kappa_0})^2$  ratio of the microstrip. ( $a = 12.7$  mm,  $d_1 = 11.43$  mm,  $d_2 = 0.5$  mm,  $d_3 = 0$  mm,  $w = 0.5$  mm,  $\epsilon_r = 9.4$ ).

#### 4. CONCLUSION

A detailed analytical development of Maxwell's equations for the characterization of a complex medium multilayer transmission line structure is presented. This study is based on the Generalized Exponential Matrix Technique combined with the method of moments and Galerkin's procedure. The analytical formulation of the problem is carried out through a matrix formulation approach that excludes all calculation complexities and avoids excessive developments of intermediate elements, in particular Equations (4c) and (13c)–(13f). This results in a compact matrix form of the Green's tensor. This matrix formulation approach facilitates the characterization study of a complex medium structure with full tensors of the constitutive parameters with the consideration, for the first time, of the substrate dielectric losses. A multitude of diverse and interesting results has been obtained, which are consistent with the literature. Among them, only the cases of exploitable applications have been interpreted.

#### ACKNOWLEDGMENT

The authors are thankful to the anonymous reviewers for making constructive criticisms on the work, which essentially helped to raise the status of manuscript.

#### REFERENCES

1. Perić, M., S. Ilić, S. Aleksić, N. Raičević, M. Bichurin, A. Tatarenko, and R. Petrov, "Covered microstrip line with ground planes of finite width," *Facta Universitatis Series: Electronics and Energetics*, Vol. 27, No. 4, 589–600, Dec. 2014.
2. Tae, H. S., K. S. Oh, H. L. Lee, W. I. Son, and J. W. Yu, "Reconfigurable 1 : 4 power divider with switched impedance matching circuits," *IEEE Microwave and Wireless Components Letters*, Vol. 22, No. 2, 64–66, Feb. 2012.
3. Koul, S. K. and B. Bhat, "Inverted microstrip and suspended microstrip with anisotropic substrates," *Proceedings of the IEEE*, Vol. 70, No. 10, 1230–1231, Oct. 1982.
4. Tsalamengas, J. L., "Interaction of electromagnetic waves with general bianisotropic slabs," *IEEE Transactions on Microwave Theory and Techniques*, Vol. 40, No. 10, 1870–1878, Oct. 1992.

5. Umashankar, K., A. Taflove, and S. Rao, "Electromagnetic scattering by arbitrary shaped three-dimensional homogeneous lossy dielectric objects," *IEEE Transactions on Antennas and Propagation*, Vol. 34, No. 6, 758–766, 1986.
6. Yin, W.-Y., L.-W. Li, and I. Wolff, "The compatible effects of gyrotropy and chirality in biaxially bianisotropic chiral-and chiroferrite-ferrite microstrip line structure," *International Journal of Numerical Modelling: Electronic Networks, Devices and Fields*, Vol. 12, 209–227, 1999.
7. Weiglhofer, W. S., "A perspective on bianisotropy and Bianisotropics' 97," *International Journal of Applied Electromagnetics and Mechanics*, Vol. 9, No. 2, 93–101, 1998.
8. Zebiri, C., D. Sayad, S. Daoudi, and F. Benabdelaziz, "Microstrip line printed on a bianisotropic medium," *International Conference on Advanced Communication Systems and Signal Processing, ICOSIP-2015*, 111–120, 2015.
9. Heindl, R., H. Srikanth, S. Witanachchi, P. Mukherjee, T. Weller, A. S. Tatarenko, and G. Srinivasan, "Structure, magnetism, and tunable microwave properties of pulsed laser deposition grown barium ferrite/barium strontium titanate bilayer films," *J. Appl. Phys.*, Vol. 101, No. 09, 09M503, 2007.
10. Tatarenko, A. S., D. V. Snisarenko, and M. Bichurin, "Modeling of magnetoelectric microwave devices," *Facta Universitatis, Series: Electronics and Energetics*, Vol. 30, No. 3, 285–293, 2017.
11. Zebiri, C., F. Benabdelaziz, and M. Lashab, "Bianisotropic superstrate effect on rectangular microstrip patch antenna parameters," *META '12*, 2012.
12. Herman, W.-N., "Polarization eccentricity of the transverse field for modes in chiral core planar waveguides," *Journal of the Optical Society of America A: Optics, Image Science and Vision*, Vol. 18, No. 11, 2806–2818, 2001.
13. Engheta, N., "The theory of chirostrip antennas," *Proceedings of the 1988 URSI International Radio Science Symposium, 213*, Syracuse, New York, 1988.
14. Zebiri, C., M. Lashab, and F. Benabdelaziz, "Effect of anisotropic magneto-chirality on the characteristics of a microstrip resonator," *IET Microwaves, Antennas Propagation*, Vol. 4, No. 4, 446–452, 2010.
15. Hillion, P., "Harmonic plane wave propagation in anisotropic chiral media," *International Journal of Applied Electromagnetics and Mechanics*, Vol. 28, No. 3, 337–350, 2008.
16. Khodja, A., M. L. Tounsi, M. C. E. Yagoub, and S. Gaoua, "Full-wave analysis of the anisotropy effect in unilateral planar transmission lines by integral method," *SETIT 2005, 3rd International Conference: Sciences of Electronic Technologies of Information and Telecommunications*, Mar. 27–31, 2005.
17. Daoudi, S., F. Benabdelaziz, and C. Zebiri, "Spectral-domain analysis of finline printed on chiral and ferrite substrates using the generalized exponential technique combined with Galerkin's method," *European Journal of Science and Technology*, No. 8, 53–56, Sep. 2016. (Special Issue of the *2nd International Conference on Computational and Experimental Science and Engineering (ICCESN-2015)*, Antalya, Turkey, Oct. 14–19, 2015.)
18. Aib, S., F. Benabdelaziz, C. Zebiri, and D. Sayad, "Propagation in diagonal anisotropic chiro-waveguides," *Advances in OptoElectronics*, Vol. 2017, 2017.
19. Lindell, V., A. H. Sihvola, S. A. Tretyakov, and A. J. Vitonen, *Electromagnetic Waves in Chiral and Bi-isotropic Media*, Altech House, Norwood, MA, 1994.
20. Wang, S. Y., W. Y. Yin, L. Zhou, J. Chen, X. Q. Gu, and L. F. Qiu, "THz wave interaction with planar structures consisting of multilayer graphene sheets and bianisotropic slabs," *IEEE International Wireless Symposium (IWS)*, 1–4, 2014.
21. Zebiri, C., F. Benabdelaziz, and M. Lashab, "Complex media parameter effect: On the input impedance of rectangular microstrip antenna," *IEEE International Conference Complex Systems (ICCS)*, 1–4, 2012.
22. Zebiri, C., M. Lashab, and F. Benabdelaziz, "Asymmetrical effects of bi-anisotropic substrate-superstrate sandwich structure on patch resonator," *Progress In Electromagnetics Research B*, Vol. 49, 319–337, 2013.

23. Tretyakov, S. A. and A. A. Sochava, "Proposed composite material for nonreflecting shields and antenna radoms," *Electron. Lett.*, Vol. 29, No. 12, 1048–1049, 1993.
24. Dmitriev, V., "Table of the second rank constitutive tensors for linear homogeneous media described by the point magnetic groups of symmetry," *Progress In Electromagnetic Research*, Vol. 28, 43–95, 2000.
25. Yin, W.-Y., "Linear complex media," *Encyclopedia of RF and Microwave Engineering*, 694–717, John Wiley, New York, 2005.
26. Zebiri, C., M. Lashab, and F. Benabdelaziz, "Rectangular microstrip antenna with uniaxial bi-anisotropic chiral substrate-superstrate," *IET Microwaves, Antennas Propagation*, Vol. 5, No. 1, 17–29, Jan. 2011.
27. Sayad, D., F. Benabdelaziz, C. Zebiri, S. Daoudi, and R. A. Abd-Alhameed, "Spectral domain analysis of gyrotropic anisotropy chiral effect on the input impedance of a printed dipole antenna," *Progress In Electromagnetics Research M*, Vol. 51, 1–8, 2016.
28. Zebiri, C., S. Daoudi, F. Benabdelaziz, M. Lashab, D. Sayad, N. T. Ali, and R. A. Abd-Alhameed, "Gyro-chirality effect of bianisotropic substrate on the operational of rectangular microstrip patch antenna," *International Journal of Applied Electromagnetics and Mechanics*, Vol. 51, No. 3, 249–260, 2016.
29. Khodja, A., M. C. E. Yagoub, R. Touhami, and H. Baudrand, "Improved numerical modal technique for fast and accurate modeling of transmission planar structures: Application to microstrip line," *2015 International Conference on Synthesis, Modeling, Analysis and Simulation Methods and Applications to Circuit Design (SMACD)*, 1–4, IEEE, 2015.
30. Polichronakis, I. P. and S. S. Kouris, "Computation of the dispersion characteristics of a shielded suspended substrate microstrip line," *IEEE Transactions on Microwave Theory and Techniques*, Vol. 40, No. 3, 581–584, 1992.